Journal of Molecular Structure 1038 (2013) 73–77

Contents lists available at SciVerse ScienceDirect

Journal of Molecular Structure

journal homepage: www.elsevier.com/locate/molstruc

Crystal structure and temperature-dependent fluorescent property of a 2D cadmium (II) complex based on 3,6-dibromobenzene-1,2,4,5-tetracarboxylic acid

Liang-Liang Zhang, Yu Guo, Yan-Hui Wei, Jie Guo, Xing-Po Wang *, Dao-Feng Sun *

Key Lab of Colloid and Interface Chemistry, Ministry of Education, School of Chemistry and Chemical Engineering, Shandong University, Jinan 250100, PR China

HIGHLIGHTS

- A new cadmium (II) coordination polymer was synthesized and characterized.
- Hydrogen bond and Br···O halogen bond interactions were observed in **1**.
- The temperature-dependent fluorescent property of **1** was investigated.

ARTICLE INFO

Article history:
Received 16 September 2012
Received in revised form 11 January 2013
Accepted 11 January 2013
Available online 31 January 2013

Keywords:
Cadmium (II) complex
Hydrogen and halogen bond
Temperature-dependent fluorescent

ABSTRACT

A new cadmium (II) organic coordination polymers $[Cd(dbtec)_{0.5}(H_2O)_3]\cdot H_2O$ (**1**), has been constructed based on 3,6-dibromobenzene-1,2,4,5-tetracarboxylic acid (H_4dbtec), and characterized by elemental analysis (EA), infrared spectroscopy (IR), powder X-ray diffraction (PXRD), and single crystal X-ray diffraction. In **1**, μ_2-η^1:η^1 and μ_4-η^2:η^2 dbtec ligands link four hepta-coordinated Cd^{II} ions to form a 2D 4^4 topological layer structure, which is further connected into an interesting 3D network by hydrogen bond and Br···O halogen bond. Moreover, the thermal stabilities, solid ultraviolet spectroscopy and temperature-dependent fluorescent properties of **1** were investigated.

1. Introduction

With the development of supermolecular chemistry and crystal engineering, the rational design and synthesis of metal-organic coordination polymers has attracted much attention, not only because of their intriguing variety of architectures and topologies but also owing to their potential applications in catalysis, gas absorption, ion exchange, luminescent and so on [1–7]. The deliberate predict and control of the topology of structure is impossible, but logical choice of the organic ligands and the central metal atoms can produce different types of coordination frameworks with novel topologies. Recently, poly-carboxylate ligands are good candidates for the assembly of versatile structures.

According to our survey of the Cambridge Structural Database (CSD), a great number of crystal structures based on 1,2,4,5-benzenetetracarboxylic acid (H_4btec) have been reported by other's group [8–11], but there is no coordination polymers based on 3,6-dibromobenzene-1,2,4,5-tetracarboxylic acid (H_4dbtec) (Scheme 1). The ligand was chosen for the remarkable advantages: (i) the ligand has four carboxyl groups, providing abundant coordination sites and modes, which may facilitate the formation of novel topologies; (ii) the multidentate ligand H_4dbtec has two bromine atoms, which could form halogen bond, directing the resulting supramolecular structure. At the same time, the luminescent properties of metal-organic frameworks (MOFs) have been intensively studied [12]. Considering these in mind, we reported a new coordination polymer based on H_4dbtec and $Cd(NO_3)_2\cdot 4H_2O$, which featured a two-dimensional 4^4 layer that was assembled into a three-dimensional framework directed by hydrogen bond and Br···O halogen bond. Moreover, the temperature-dependent fluorescent property of **1** was also investigated.

2. Experimental procedure

2.1. Materials and methods

All the reagents and solvents employed were commercially available and used as received without further purification except H_4-dbtec. Infrared spectra were recorded on a Bruker VERTEX-70 spectrometer as KBr pellets in the frequency range 4000–400 cm^{-1}. The elemental analyses (C, H contents) were determined on a CE instruments EA 1110 analyzer. Photoluminescence measurements were performed on a Hitachi F-7000 fluorescence spectrophotometer

* Corresponding authors. Fax: +86 531 88364218.
E-mail address: dfsun@sdu.edu.cn (D.-F. Sun).

0022-2860/$ - see front matter © 2013 Elsevier B.V. All rights reserved.
http://dx.doi.org/10.1016/j.molstruc.2013.01.027

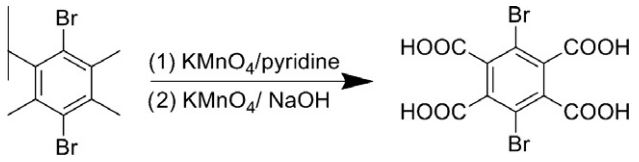

Scheme 1. The reaction pathway of H_4dbtec.

with solid powder on a 1 cm quartz round plate with a dewar flask apparatus. TG curves were measured from 30 to 600 °C on a SDT Q600 instrument at a heating rate 10 °C/min under the N_2 atmosphere (100 mL/min). Solid-state UV–vis diffuse reflectance spectra was obtained at room temperature using agilent Cary 100 spectrophotometer, and $BaSO_4$ was used as a 100% reflectance standard for all materials.

2.2. Synthesis of H_4dbtec ligand

The reaction pathway is shown in Scheme 1. H_4dbtec ligand was prepared according literature [13] and with a little modification. To a four-necked flask equipped with a reflux condenser and a mechanical stirrer, 3,6-bromo-tetramethylbenzene (0.171 mol), 2.1 L pyridine and 280 mL water were added. The reaction mixture was heated to 100 °C while stirring. $KMnO_4$ (0.859 mol) was added in small portions and the mixture was refluxed for 5 h. The warm solution was separated from MnO_2 by filtration and the solvent evaporated under reduced pressure. 280 mL water and 112 g NaOH were added to the residual solid. After the combined mixture was heated up to 100 °C, $KMnO_4$ (0.859 mol) was added again in small portions and the mixture was refluxed for 5 h. The excess $KMnO_4$ was destroyed by the cautious addition of 140 mL ethanol. The MnO_2 was removed from the hot mixture by filtration. The filtrate was acidified with aqueous HCl (5 M, 600 mL). After the solvent was revaporated, the residue was washed with acetone. The resultant solid was dried. The yield was 46 g (66%). ^{1}H NMR (300 MHz; DMSO-d_6) no signals. ^{13}C NMR (100 MHz; DMSO-d_6) δc 115.51, 137.57, 166.27.

2.3. Synthesis of $[Cd(dbtec)_{0.5}(H_2O)_3]\cdot H_2O$ (**1**)

The new complex (**1**) was prepared by liquid diffusion method. In a 18 × 180 mm test tube, $Cd(NO_3)_2\cdot 4H_2O$ (0.05 mmol, 15 mg) in 5 mL of ethanol was layered onto a solution of 3,6-dibromobenzene-1,2,4,5-tetracarboxylic acid (H_4dbtec) (0.05 mmol, 20 mg) in 10 mL H_2O. The resulting mixture was kept at room temperature, and colorless rod-like crystals were obtained after 3 weeks. Yield: 56%. Elemental analyses for $C_5H_8BrCdO_8$ (387.42): Calcd. C 15.46; H 2.08%; found: C 15.64; H 2.37%. Selected IR peaks (cm^{-1}): 3563 (s), 2922 (w), 1609 (s), 1431 (m), 1384 (m), 1329 (s), 1129 (m), 890 (m), 836 (w), 776 (w), 709 (w), 654 (w), 576 (w), 513 (w), 422 (w).

2.4. X-ray crystallography

Single crystals of the complex **1** with appropriate dimensions was chosen under an optical microscope and quickly coated with high vacuum grease (Dow Corning Corporation) before being mounted on a glass fiber for data collection. Data for **1** was collected on a Bruker SMART APEX II CCD diffractometer with graphite-monochromated MoKα radiation source (λ = 0.71073 Å) operating at 50 kV and 40 mA by using a multi-scan technique at room temperature. A preliminary orientation matrix and unit cell parameters were determined from 3 runs of 12 frames each, each frame corresponds to a scan in 5 s, followed by spot integration and least-squares refinement. Data were measured using ω scans for 10 s per frame until a complete hemisphere had been collected. Cell parameters were retrieved using SMART software and refined with SAINT on all observed reflections. Data reduction was performed with the SAINT software and corrected for Lorentz and polarization effects. Absorption corrections were made using the SADABS program [14]. The structures were solved using direct methods and successive Fourier difference synthesis (SHELXS-97) [15] and they were refined using the full-matrix least-squares method on F^2 with anisotropic thermal parameters for all non-hydrogen atoms (SHELXL-97) [16]. Atoms were located from iterative examination of difference F-maps following least squares refinements of the earlier models. Hydrogen atoms were placed in calculated positions and included as riding atoms with isotropic displacement parameters 1.2–1.5 times *U*eq of the attached C atoms. Structure was examined using the Addsym subroutine of PLATON [17] to assure that no additional symmetry could be applied to the models. For **1**, crystal data and collection and parameters are summarized in Table 1, and selected bond lengths and angles are given in Table 2.

3. Results and discussion

3.1. Syntheses and IR

H_4dbtec ligand was synthesized by oxidation reaction of 3,6-bromo-tetramethylbenzene with $KMnO_4$ as an oxidant. The purity of H_4dbtec ligand has been detected by ^{1}H and ^{13}C NMR (Fig. S1). Crystallization of the complex **1** was carried out in liquid diffusion method at room temperature. As shown in Fig. S2, the observed broad peak at 3500 cm^{-1} in the FT-IR spectrum is attributed to the O—H stretching vibration of the coordinated water molecules and the characteristic asymmetric (ν_{as}) and symmetric (ν_s) absorptions of the carboxylate groups appear as strong bands at about 1600 and 1400 cm^{-1}, respectively. The absence of the characteristic bands at ~1700 cm^{-1} attributed to the carboxyl groups indicated the complete deprotonation of all carboxyl groups in **1** upon reaction with Cd^{II} ions [18–20]. In order to descript the correction between structure and temperature, IR spectrum was performed by using the same sample but at different temperature (room temperature 298 K and low temperature 77 K). As shown in Fig. S2, The IR absorption peak of **1** at room temperature is

Table 1
Crystallographic data for **1**.

Empirical formula	$C_5H_8BrCdO_8$
Formula weight	387.42
Temperature (K)	273.15
Crystal system	Monoclinic
Space group	$P2_1/n$
a (Å)	10.115(6)
b (Å)	6.421(4)
c (Å)	15.545(9)
α (°)	90.00
β (°)	97.435(9)
γ (°)	90.00
Volume (Å^3)	1001.1(10)
Z	4
ρ_{calc} (mg/mm^3)	2.570
m/mm^{-1}	6.194
F(000)	736.0
2Θ range for data collection	4.54–49.98°
Index ranges	$-11 \leqslant h \leqslant 12$, $-6 \leqslant k \leqslant 7$, $-18 \leqslant l \leqslant 15$
Reflections collected	4679
Independent reflections	1760[*R*(int) = 0.0253]
Data/restraints/parameters	1760/0/137
Goodness-of-fit on F^2	1.062
Final *R* indexes [$I \geqslant 2\sigma$ (*I*)]	R_1 = 0.0254, wR_2 = 0.0651
Final *R* indexes (all data)	R_1 = 0.0289, wR_2 = 0.0669
Largest diff. peak/hole (*e* Å^{-3})	0.66/−0.64

Table 2
Selected bond distances (Å) and angles (°) for **1**.

Cd—O1^{i}	2.233 (3)	O2W—Cd—O4	89.15 (12)
Cd—O2W	2.238 (3)	O3—Cd—O4	55.35 (10)
Cd—O3	2.315 (3)	O3W—Cd—O4	90.32 (12)
Cd—O3W	2.324 (3)	O1^{i}—Cd—O4W	93.90 (12)
Cd—O4	2.370 (3)	O2W—Cd—O4W	82.73 (12)
Cd—O4W	2.400 (3)	O3—Cd—O4W	81.30 (11)
O1—Cd^{ii}	2.233 (3)	O3W—Cd—O4W	169.96 (12)
O1^{i}—Cd—O2W	88.39 (13)	O4—Cd—O4W	84.28 (12)
O1^{i}—Cd—O3	126.67 (11)	O1^{i}—Cd—C5	154.28 (13)
O2W—Cd—O3	142.20 (11)	O3W—Cd—C5	97.18 (12)
O1^{i}—Cd—O3W	91.13 (13)	O4—Cd—C5	27.70 (12)
O2W—Cd—O3W	88.75 (11)	O4W—Cd—C5	81.92 (11)
O3—Cd—O3W	102.57 (11)	O1^{i}—Cd—O4	177.09 (12)

Symmetry code [i: $1-x$, $-y$, $1-z$; ii: $1/2+x$, $-1/2-y$, $-1/2+z$; iii: $1/2-x$, $-1/2+y$, $3/2-z$].

broadly similar to that of low temperature, but the transmittance measured in low temperature is much stronger than that of room temperature, which maybe attribute to the rigidity of ligands and shortening of bond length at low temperature.

3.2. Crystal structure of $[Cd(dbtec)_{0.5}(H_2O)_3]\cdot H_2O$ (**1**)

Single-crystal X-ray diffraction analysis reveals that each Cd^{II} ion is hepta-coordinated by four carboxylate oxygen atoms from two different dbtec molecules and three oxygen atoms from three coordinated water molecules. As shown in Fig. 1, complex **1** crystallizes in monoclinic $P2_1/n$ space group with an asymmetric unit containing one crystallographic independent Cd^{II} ion, half H_4dbtec ligand, three coordinated and one lattice water molecules. The Cd—O_{dbtec} distances range from 2.233 (3) to 2.370 (3) Å and Cd—O_w distances range from 2.238 (3) to 2.400 (3) Å. The bond angles O—Cd—O range from 55.37 (10) to 177.14 (12)°, which are comparable to those of reported Cd^{II} coordination polymers [21–23]. Because of the synergistic effect of electronic and steric hindrance effect between Br and carboxylate group, dihedral angles between carboxylate group and central benzene rings are in the range 67.610 (17)–71.024 (14)°. The Cd^{II} ion in **1** adopts distorted pentagonal bipyramids geometry. Four carboxylate groups of the dbtec ligand exhibit two kinds of coordination modes: each of two *para*-carboxylate groups adopts monodentate mode, coordinating to one cadmium atom whereas each of the other two *para*-carboxylate groups exhibits a chelating bridging mode linking one cadmium atom, which produces a 2D layered structure (Fig. 2a). To better understand the complicated structure of **1**, the topological analysis of complex **1** has been performed using OLEX [24]. The individual two-dimensional motif can be simplified as a 4^4 topological layer if the dbtec ligand is simplified as a four-connected node (Fig. 2b).

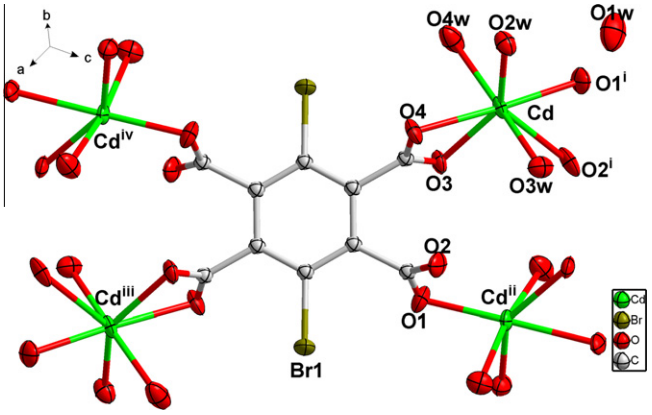

Fig. 1. The coordination environment of the Cd^{II} ions and the linkage modes of H_4dbtec ligands in **1** with 50% thermal ellipsoid probability, hydrogen atoms are omitted for clarity. (i: $1.5-x$, $0.5+y$, $1.5-z$; ii: $1.5-x$, $-0.5+y$, $1.5-z$; iii: $2-x$, $1-y$, $1-z$; iv: $0.5+x$, $1.5-y$, $-0.5+z$).

Hydrogen and halogen bonds were also investigated, because the weak forces were suggested to act as a structure-direction tool [25–26]. In complex **1**, the coordinated and uncoordinated H_2O provided potential hydrogen-bond donors and acceptors. In complex **1**, hydrogen-bond can also be observed between carboxylate oxygen atoms and coordinated water molecules. The detailed hydrogen-bonding parameters are listed in Table 3. At the same time, Br···O halogen bonds connected adjacent two-dimensional layers with Br···$O2_W$ distance of 3.198(4) Å and Br···$O1_W$ range from 3.563(8) to 3.567(4) Å. The angle $\Theta 1$ ($\angle$C—Br···$O2_W$) was 60.891(11)°, the geometrical characteristics of Br···O interactions may be understood that by assigning a positive polarization in the polar region of the Br atom and a negative polarization in its equatorial region. Meanwhile, intramolecular Br···O halogen bonds existed with the distance between 3.334(3) and 3.339(6) Å. Moreover, weak hydrogen-bonds ($O1_W$—$H1_{WB}$···Br) were also observed. Because of the hydrogen bonds and halogen bonds mentioned above, the structure changed from 2D layer to an interesting 3D framework (Fig. 2c). As shown in Fig. 3, the layer grids consist of a kind of large 30-membered-ring hole which contains four H_4dbtec ligands and four Cd^{II} ions. As far as we know, Yang et. al reported a complex based on btec units and binuclear Cd^{II} ions, producing a step-like 2D layered structure, which contained 14-membered-ring and 16-membered-ring holes [27]. Based on the structure comparison of H_4dbtec and H_4btec ligands, we concluded that not only the steric hindrance but also the electronic effect of Br impacted the coordination preferences of the dbtec units, consequently, different structural motifs were produced. Meanwhile, coexistent hydrogen bond and Br···O halogen bonds strengthen interactions between adjacent layers and play important roles in the formation of the resulting 3D supramolecular frameworks.

3.3. X-ray Power Diffraction Analyses and Thermogravimetric Analyses

In order to check the phase purities of **1**, the X-ray powder diffraction patterns of them was recorded at room temperature. As shown in Fig. S3, the peak positions of simulated and experimental patterns are in good agreement with each other, demonstrating the phase purity of the product. The dissimilarities in intensity may be due to the preferred orientation of the crystalline powder samples.

The thermal behavior of **1** was studied by TGA (Fig. 4). The experiments were performed on the samples consisting of numerous single crystals under N_2 atmosphere with a heating rate of 10 °C min^{-1}. The TGA curve of **1** displays two step decomposition, corresponding to the loss of lattice and coordinated water molecules (Calcd. 18.4%, Found 17.8%). The decompositions start at 335 °C for **1**, accompanying the release of the dbtec ligands. The relative high thermal stability of **1** may be attributed to its 2D dimensionality connected by hydrogen bond and Br···O halogen bond.

3.4. UV–vis absorption and photoluminescence properties

The UV–vis absorption spectra of compounds **1** was obtained in the solid-state at room temperature. As shown in Fig. S4, compounds **1** shows intense absorption peaks at 230–320 nm, which can be ascribed to ($\pi \rightarrow \pi^*$) transitions of the ligands. Luminescent properties of d^{10} transition metal complexes have been well reported. The organic ligands, their coordination modes and temperature have great effect on the emission wavelengths and luminescent mechanisms. In order to well understand the luminescent property of complex **1**, the temperature-dependent spectrum of

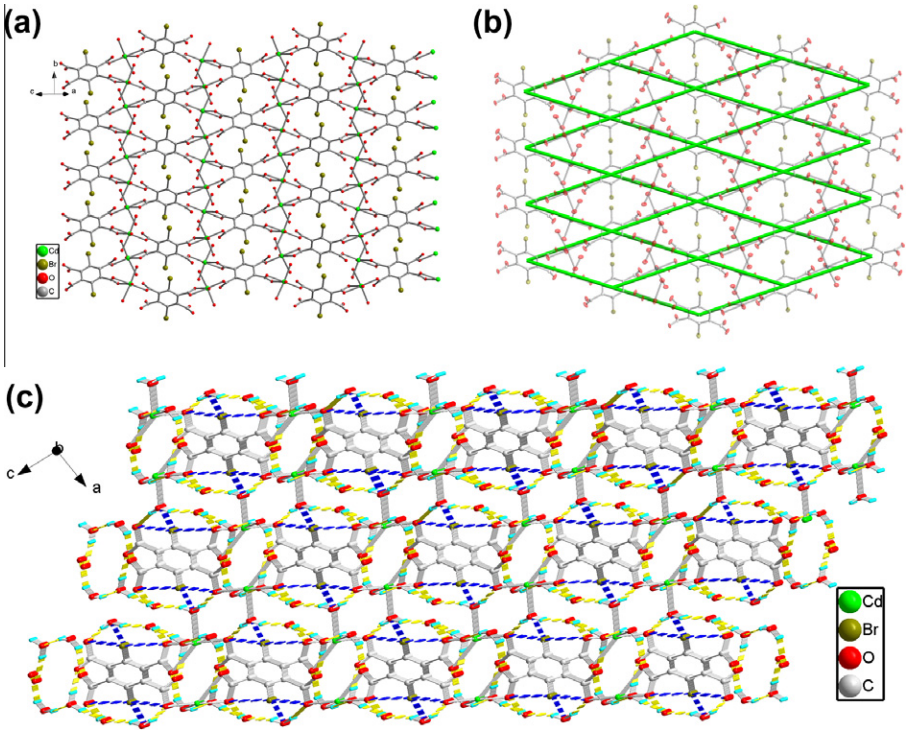

Fig. 2. (a) The 2D layer structure between Cd^{II} and ligands. (b) Schematic representation of the 4-connected 4^4 layer. (c) Hydrogen bonds and halogen bond induced 2D–3D framework (yellow and blue dotted lines represent hydrogen bonds and halogen bond, respectively). (For interpretation of the references to colour in this figure legend, the reader is referred to the web version of this article.)

Table 3
Hydrogen-bonding geometrical parameters/Å, ° for compound **1**.

D—H···A	D—H	H···A	D···A	∠D—H···A
O2W—H2WA···O1W	0.85	1.90	2.702 (5)	157.5
O2W—H2WB···O4^{i}	0.85	1.86	2.700 (4)	171.6
O3W—H3WA···O3^{ii}	0.85	1.91	2.749 (4)	168.7
O3W—H3WB···O1W^{iii}	0.85	2.22	2.978 (6)	148.6
O4W—H4WA···O3W^{iv}	0.85	2.03	2.852 (5)	163.2
O4W—H4WB···O2^{iv}	0.85	2.13	2.884 (5)	147.4
O1W—H1WA···O1^{v}	0.85	1.95	2.746 (5)	156.2
O1W—H1WB···O1^{vi}	0.85	2.18	2.983 (5)	157.1

Symmetry codes: (i) $-x, -y, -z+1$; (ii) $-x+1/2, y-1/2, -z+3/2$; (iii) $-x-1/2, y-1/2, -z+3/2$; (iv) $x, y+1, z$; (v) $x-1, y, z$; (vi) $-x+1/2, y+1/2, -z+3/2$.

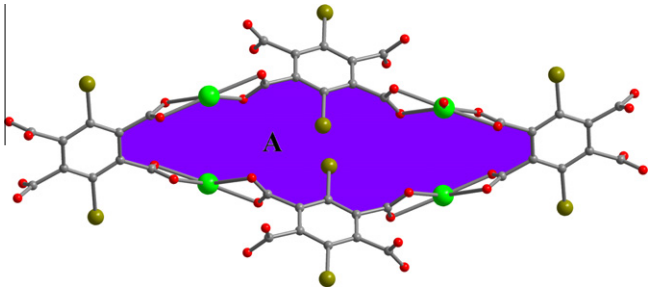

Fig. 3. The 30-member-ring in complex **1** labeled A.

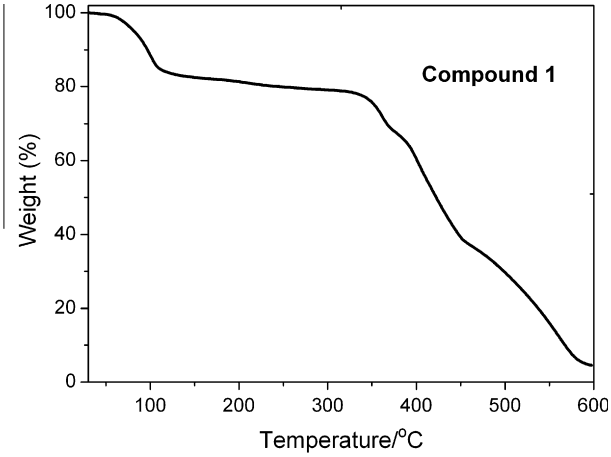

Fig. 4. TGA curve of **1**.

complex **1** and free ligand (H_4dbtec) were measured at room temperature (298 K) and low temperature (77 K) Fig. 5. The solid-state emission spectrum of **1** and H_4dbtec at room temperature displays an emission band centered at 464 nm and 471 nm with excitation maximum at 310 nm. As the temperature is decreased to 77 K, a blue shift of 14 nm and surprising fluorescence enhancement is observed with respect to the emission band of **1** at room temperature, suggesting its high sensitivity to temperature. The emission of H_4dbtec was ascribed to the $\pi^* \rightarrow n$ or $\pi^* \rightarrow \pi$ electronic transitions [28–30]. Because the Cd^{II} ion is difficult to oxidize or to reduce due to its d^{10} electronic configuration, the emissions of these complexes are neither metal-to-ligand charge transfer nor ligand-to-metal charge transfer. The emission of complex **1** can be assigned to the intraligand or ligand-to-ligand charge transition as a result of the resemblance of the emission spectra in comparison with those of the free ligand [31–32]. The increase in fluorescence can be attributed to the rigidity of ligands which is favorable for cold conditions, with the decrease of radiationless decay process of the intraligand ($\pi \rightarrow \pi^*$) excited state [33].

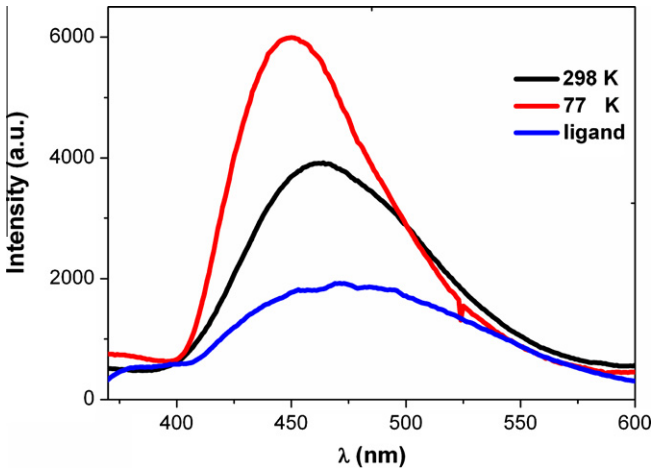

Fig. 5. Temperature-dependent emission spectra of **1** and free ligand.

4. Conclusions

A new Cd^{II} compound was synthesized and characterized. Compound **1** crystallized in 2-dimensional 4^4 topological layer and features an interesting 2D–3D framework directed by hydrogen bonds and Br···O halogen bonds. Meanwhile, in complex **1**, there was a kind of large 30-member-ring hole which contained four H_4dbtec ligands and four Cd^{II} ions. The temperature-dependent solid-state luminescent property of complex **1** showed blue shift both under ambient and freezing conditions, and drastic fluorescence enhancement when the temperature was lowered.

Acknowledgments

This work was supported by the NSFC (Grant No. 90922014), the Shandong Natural Science Fund for Distinguished Young Scholars (2010JQE27021), the NSF of Shandong Province (BS2009L007 and Y2008B01), Independent Innovation Foundation of Shandong University (2010JQ011).

Appendix A. Supplementary material

The Crystallographic data (excluding structure factors) for the structures in this paper have been deposited with the Cambridge Crystallographic Data Centre, CCDC, 12 Union Road, Cambridge CB21EZ, UK. Copies of the data can be obtained free of charge on quoting the depository numbers CCDC-887994 (Fax: +44-1223-336-033; E-Mail: deposit@ccdc.cam.ac.uk, http://www.ccdc.cam.ac.uk). Supplementary data associated with this article can be found, in the online version, at http://dx.doi.org/10.1016/j.molstruc.2013.01.027.

References

[1] S. Leininger, B. Olenyuk, P.J. Stang, Chem. Rev. 100 (2000) 853–908.
[2] S.H. Feng, R.R. Xu, Acc. Chem. Res. 34 (2001) 239–247.
[3] X.M. Zhang, M.L. Tong, X.M. Chen, Angew. Chem. Int. Ed. 41 (2002) 1029–1031.
[4] B.L. Chen, Y.Y. Ji, M. Xue, F.R. Fronczek, E.J. Hurtado, J.U. Mondal, C.D. Liang, S. Dai, Inorg. Chem. 47 (2008) 5543–5545.
[5] G. Ferey, C. Mellot-Draznieks, C. Serre, F. Millange, Acc. Chem. Res. 38 (2005) 217–225.
[6] D. Sun, N. Zhang, R.B. Huang, L.S. Zheng, Cryst. Growth Des. 10 (2010) 3699–3709.
[7] D. Sun, L.L. Zhang, Z.H. Yan, D.F. Sun, Chem. Asian J. 7 (2012) 1558–1561.
[8] C. Volkringer, T. Loiseau, N. Guillou, G. Ferey, M. Haouas, F. Taulelle, N. Audebrand, I. Margiolaki, D. Popov, M. Burghammer, C. Riekel, Cryst. Growth Des. 9 (2009) 2927–2936.
[9] C. Volkringer, T. Loiseau, N. Guillou, G. Ferey, M. Haouas, F. Taulelle, E. Elkaim, N. Stock, Inorg. Chem. 49 (2010) 9852–9862.
[10] K. Koh, A.G. Wong-Foy, A.J. Matzger, Angew. Chem. Int. Ed. 47 (2008) 677–680.
[11] Q.F. Yang, Y. Yu, T.Y. Song, J.H. Yu, X. Zhang, J.Q. Xu, T.G. Wang, CrystEngComm. 11 (2009) 1642–1649.
[12] Y.J. Cui, Y.F. Yue, G.D. Qian, B.L. Chen, Chem. Rev. 112 (2012) 1126–1162.
[13] T.H. Rhee, T. Choi, E.Y. Chung, Macromol. Chem. Phys. 202 (2001) 906–910.
[14] Bruker. SMART, SAINT and SADABS. Bruker AXS Inc., Madison, Wisconsin, USA, 1998.
[15] G.M. Sheldrick, SHELXS-97, Program for X-ray Crystal Structure Determination, University of Göttingen, Germany, 1997.
[16] G.M. Sheldrick, SHELXL-97, Program for X-ray Crystal Structure Refinement, University of Göttingen, Germany, 1997.
[17] A.L. Spek, Implemented as the PLATON Procedure, a Multipurpose Crystallographic Tool, Utrecht University, Utrecht, The Netherlands, 1998.
[18] F.N. Dai, H.Y. He, D.F. Sun, J. Am. Chem. Soc. 130 (2008) 14064–14065.
[19] S.L. Cai, S.R. Zheng, Z.Z. Wen, J. Fan, N. Wang, W.G. Zhang, Cryst. Growth Des. 12 (2012) 4441–4449.
[20] M. Ahmad, R. Das, P. Lama, P. Poddar, P.K. Bharadwaj, Cryst. Growth Des. 12 (2012) 4624–4632.
[21] X.L. Zhao, L.L. Zhang, H.Q. Ma, D. Sun, D.X. Wang, S.Y. Feng, D.F. Sun, RSC Adv. 2 (2012) 5543–5549.
[22] H.Y. He, H.D. Yin, D.Q. Wang, H.Q. Ma, G.Q. Zhang, D.F. Sun, Eur. J. Inorg. Chem. 30 (2010) 4822–4830.
[23] T. Hu, L. Liu, X. Lv, X. Chen, H. He, F. Dai, G. Zhang, D. Sun, Polyhedron 29 (2010) 296–302.
[24] O.V. Dolomanov, A.J. Blake, N.R. Champness, M. Schröder, OLEX: new software for visualization and analysis of extended crystal structures, J. Appl. Crystallogr. 36 (2003) 1283–1284.
[25] F. Li, X. Zhang, Y.G. Yao, Z. Anorg, Allg. Chem. 638 (2012) 688–691.
[26] O. Takahashi, Y.J. Kohno, M. Nishi, Chem. Rev. 110 (2010) 6049–6076.
[27] Y.Q. Sun, J. Zhang, G.Y. Yang, J. Coord. Chem. 57 (2004) 1299–1308.
[28] P. Metrangolo, F. Meyer, T. Pilati, G. Resnati, G. Terraneo, Angew. Chem. Int. Ed. 47 (2008) 6114–6127.
[29] D. Sun, R.B. Huang, L.S. Zheng, J. Chem. Sci. 66 (2011) 1035–1041.
[30] X.L. Zhao, X.Y. Wang, S.N. Wang, J.M. Dou, P.P. Cui, Z. Chen, D. Sun, X.P. Wang, D.F. Sun, CrystEngComm. 12 (2012) 2736–2739.
[31] D. Sun, Z.H. Wei, D.F. Wang, N. Zhang, R.B. Huang, L.S. Zheng, Cryst. Growth Des. 11 (2011) 1427–1430.
[32] D. Sun, H.R. Xu, C.F. Yang, Z.H. Wei, N. Zhang, R.B. Huang, L.S. Zheng, Cryst. Growth Des. 10 (2010) 4642–4649.
[33] Q.L. Zhu, C.J. Shen, C.H. Tan, T.L. Sheng, S.M. Hua, X.T. Wu, Chem. Commun. 48 (2012) 531–533.